Preparation of spinel $Li_{1.06}Mn_2O_{4-z}Cl_z$ cathode materials by the citrate gel method

Wen-Ren Liu [a], She-Huang Wu [a,*], Hwo-Shuenn Sheu [b]

[a] *Department of Materials Engineering, Tatung University, 40 Chungshan N. Rd., Sec.3, Taipei 104, Taiwan Roc*
[b] *National Synchrotron Research Center, 1 R&D Rd. VI, Industrial Park, Hsinchu 300, Taiwan Roc*

Abstract

Chlorine-substituted spinels, $Li_{1.06}Mn_2O_{4-z}Cl_z$ with $0 \leq z \leq 0.10$, were prepared with a citrate gel method to investigate the effects of Cl-doping on the crystal structure and the properties as cathode material for lithium-ion batteries. Exclusive spinel phase were found in the prepared powders. The lattice parameter of spinel increases from 8.227 Å for $z = 0$ to 8.238 Å for $z = 0.06$ and becomes saturated for $0.06 < z < 0.10$. It indicates chlorine has been successfully doped into the spinel structure. The sample with $z = 0.06$ shows better cycling performance than that of others. The initial specific discharge capacity of 123 mAh g^{-1} and capacity loss rate of 0.21 mAh g^{-1} cycle^{-1} was measured for these samples. Variation in the crystal structure during charge/discharge was examined with in situ XRD. Two-phase coexistence was observed at voltage between 4.15 and 4.175 V.
© 2005 Elsevier B.V. All rights reserved.

Keywords: Spinel oxychloride; Cl-substituted spinel; Cathode material; In situ XRD

1. Introduction

The spinel-structured lithium manganese oxide and its derivatives have been studied extensively as 4 V cathode materials for Li-ion batteries because of their low cost and environmental benign [1–4]. However, it is suffered from a progressive capacity loss upon cycling, particularly at elevated temperatures [4–6]. The major factors responsible for the capacity loss in 4 V range are: (i) instability of the two-phase structure in the high voltage region [4,5]; (ii) manganese dissolution due to acid attack and disproportionation reaction [4–7]; (iii) reactions between electrolyte and spinel electrode in the charged state [4,8].

To improve the cycle performance, numerous studies have been made to investigate the effects of adding excess lithium to the stoichiometric $LiMn_2O_4$ spinel and substituting a small fraction of the manganese ions with other metal cations, such as Al, Ni, Cr and Co, on diminution in capacity loss [9–14]. Some of these efforts showed substantial reduction in ca-

pacity fade and improvement in reversible capacity at ambient temperature. The improvement is attributed to the increase in the average oxidation state of manganese [9–11], smaller lattice parameter and smaller volume change during lithium-ion intercalation/de-intercalation than un-substituted one [13–15]. It had also been shown that the elevated-temperature performance of Co-substituted spinel can be improved by use of low acidity electrolyte solution [13]. However, the effects on the reduction in capacity loss at elevated temperatures are not significant. Amatucci et al. [15,16] had shown that the introduction of anion substitution in the form of spinel oxyfluorides can reduce the average Mn oxidation state and improves the chemical and structural stability upon cycling. The F-substituted spinel cannot only suppress the capacity fade at elevated temperatures but also compensate the theoretical capacity reduction caused by cation substitution.

Sun et al. [17–19] reported that sulfur-doped spinel materials prepared by sol–gel method showed excellent cycle performance in both 4 and 3 V regions at room temperatures by retaining to their original cubic spinel phase at all the operating voltage regions. In addition, spinel oxysulfide with composition of $LiAl_{0.18}Mn_{1.82}O_{3.97}S_{0.03}$

---

* Corresponding author. Tel.: +886 2 25922458; fax: +886 2 25936897.
E-mail address: shwu@ttu.edu.tw (S.-H. Wu).

showed excellent cycleability in 4 V range at elevated temperatures [20]. The capacity loss for the spinel oxysulfide cycled at 80 °C was attributed to the formation of tetragonal $Li_2Mn_2O_4$ and rock salt Li_2MnO_3. Kang and Goodenough [21] had tried to decorate the $LiMn_2O_4$ spinel surface with Cl instead of S by preparing $LiMn_2O_4$ with $Li(CH_3COO)\cdot2H_2O$, $Mn(CH_3OO)_2\cdot4H_2O$ and $MnCl_2$ (in molar ratio of 1:1.85:0.15) as the staring materials, glycolic acid as chelating agent by a sol–gel method. Although no chlorine was found in the prepared powder, thus prepared spinel showed good capacity retention in the 3 V range. However, it exhibited inferior performance than the $LiMn_2O_4$ synthesized without $MnCl_2$, which had been prepared for comparison.

Here we report the synthesis and electrochemical performance at room/elevated temperatures of the chlorine-doped spinel materials, $Li_{1.06}Mn_2O_{4-z}Cl_z$, $0 \leq z \leq 0.10$. In situ XRD was also carried out to investigate the structure integrity of the oxychloride host.

2. Experimental

Spinel oxychlorides $Li_{1.06}Mn_2O_{4-z}Cl_z$, $0 \leq z \leq 0.10$, were prepared by a sol–gel method using citric acid as a chelating agent. $LiNO_3$, $LiCl$ and $Mn(NO_3)_2\cdot6H_2O$ in stoichiometric quantities were mixed in ethanol. Ethanol solution of citric acid was added to the continuously stirred solution. The resultant solution was evaporated at 80 °C until dry gel was obtained. The resulting gels were decomposed at 300 °C for 2 h and calcined at 750 °C for 4 h in air. Then the powders were cooled to 400 °C with rate of -1 °C min^{-1} followed by oven cooling. Powder X-ray diffraction (Shimadzu, XRD 6000) with Cu Kα radiation was used to identify the crystalline phases and the obtained patterns were used to determine the lattice parameters of the prepared powders with the computer software CELREF Version 3.

Cathodes were prepared by mixing 80% $Li_{1.06}Mn_2O_{4-z}Cl_z$ active powders with 13% acetylene black (Strem) and 7% polyvinylidene fluoride binder (Kynar 740, ELF) in N-methyl-pyrrolidinone (ISP). The solutions were then tape-cast on aluminum foil and dried for 1 h at 100 °C. The tapes were punched into disks with diameter of 10.0 mm, followed by pressing and drying at 110 °C for 12 h. The prepared cathodes were used to fabricate the 2032 coin cells in an Ar-filled glove box with lithium foil (FMC) anode, Celgard 2400 separator (Hoechst), and electrolyte of 1 M $LiPF_6$ in a 1:1 mixture of EC (ethylene carbonate) and DEC (diethyl carbonate). The cells were cycled galvanostatically in the voltage range of 3.6–4.3 V at a current rate of $C/3$ (0.1 mA) at ambient temperature and 55 °C.

In situ XRD studies for the $Li_{1.06}Mn_2O_{3.94}Cl_{0.06}$ cathode were performed by using the synchrotron radiation light source with wavelength of $\lambda = 1.32633$ Å on the beam line BL17A at the NSRRC in Taiwan. A single crystal of Si(1 1 1) was used as a monochromator to adjust the light energy into

the hutch. The optics was designed to focus the beam into a 0.5 mm × 2 mm spot size at the sample position. Data were collected with transmission geometry, where the synchrotron X-rays pass through the cell. A flat imaging plane (Fuji, 20 cm × 40 cm) was used as a 2D area detector, which can collect all of the in situ XRD patterns. The diffraction patterns were read out by a MAC IPR420 off line imaging plate scanner with step size of 0.02° for the 2θ scan. Aluminum is used as internal standard throughout the experiment. The cells with Kapton windows for in situ XRD studies were prepared in the similar way as coin cells, then charged/discharged to various voltages and hold for 48 h to reach quasi-equilibrium during the second cycle.

3. Results and discussion

The XRD patterns of the prepared $Li_{1.06}Mn_2O_{4-z}Cl_z$ powders are shown in Fig. 1. Spinel phase is exclusively observed with no second phase. The calculated lattice parameter increases with increasing amount of chlorine substitution in a sigmoid curve as shown in Fig. 2 and becomes saturated at $z = 0.06$. The increase in lattice parameter with chlorine substitution may be partly due to the reduction of Mn^{4+} to the larger Mn^{3+} cations, which should result in improved capacity as reported by Amatucci et al. [15]. However, the effect should be smaller than the observed changes since the amount of chlorine substitution is much lower than that of fluorine substitution for similar increment in lattice parameter reported previously [15]. The increase may be attributed predominantly to the substitution of O^{2-} (1.26 Å) by the larger Cl^- anions (1.67 Å). The saturation in lattice parameter at $z = 0.06$ may be related with the amount of lithium excess in the host spinel. As the amount of chlorine substitution is higher than 0.06, Cl^- ions may form salts instead of entering spinel phase. This will be supported by the results of capacity retention study.
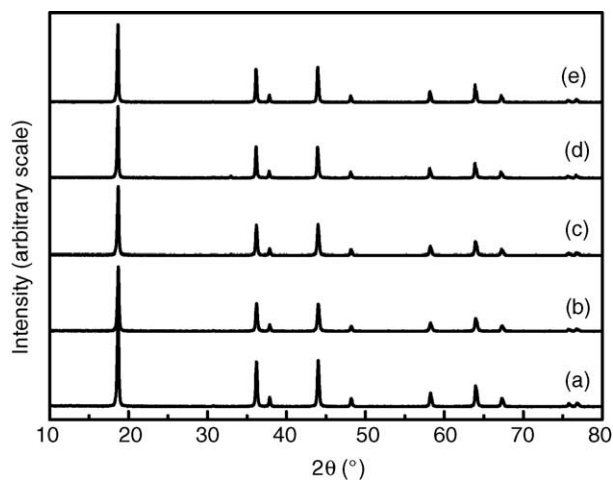

Fig. 1. XRD patterns of the prepared $Li_{1.06}Mn_2O_{4-z}Cl_z$ powders: (a) $z = 0$, (b) $z = 0.02$, (c) $z = 0.04$, (d) $z = 0.06$ and (e) $z = 0.10$.
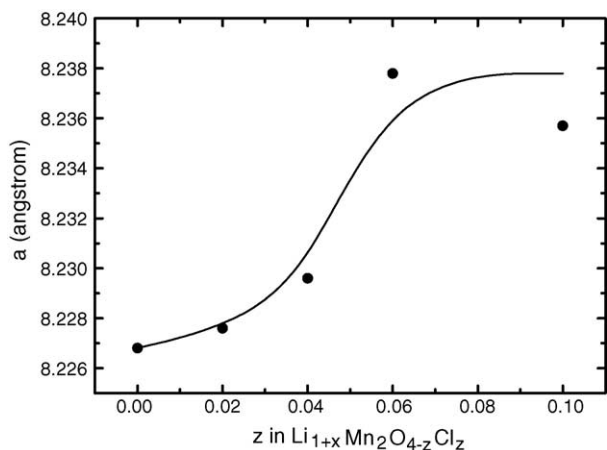
Fig. 2. Variation of spinel lattice parameter with amount of chlorine substitution.

Fig. 4. Variations of discharge capacity with cycle number for cells with various $Li_{1.06}Mn_2O_{4-z}Cl_z$ ($0 \leq z \leq 0.10$) cathodes at room temperature.

The typical charge/discharge curves of the prepared spinel oxychlorides are shown in Fig. 3. Two voltages plateaus those are the characteristics of spinel are observed at 4.0 and 4.15 V. Results of capacity retention study performed at room temperature are plotted in Fig. 4. It is found that the initial specific discharge capacity increases with amount of chlorine substitution and shows a maximum at $z = 0.06$. The increase in initial specific capacity may be caused by the increase in Mn^{3+}/Mn^{4+} ratio in the prepared powders as O^{2-} is partially substituted by Cl^- anion. As the amount of chlorine substitution is higher than 0.06, the excess chlorine may forms salts, such as LiCl, which are too low in concentration to be detected by XRD, instead of entering spinel structure and thus the specific capacity is reduced slightly. However, all of the prepared spinel oxychlorides show similar rate of capacity fade. The $Li_{1.06}Mn_2O_{3.94}Cl_{0.06}$ sample shows initial specific discharge capacity of 123 mAh g^{-1} and capacity fading rate of 0.1 mAh g^{-1} cycle^{-1}. For comparison, the results of capacity retention study for $LiMn_2O_4$ and $Li_{1.06}Mn_2O_{3.94}Cl_{0.06}$ cathodes cycled at room temperature and 55 °C are displayed

in Fig. 5. $Li_{1.06}Mn_2O_{3.94}Cl_{0.06}$ cathode does not only show superior in cycling performance to $LiMn_2O_4$ at room temperature, but also shows much lower capacity fading rate than that of $LiMn_2O_4$ at 55 °C. It demonstrates initial discharge capacity of 121 mAh g^{-1} and capacity fading rate of 0.25 mAh g^{-1} cycle^{-1}, whereas the $LiMn_2O_4$ shows initial specific discharge capacity of 131 mAh g^{-1} and capacity fading rate of 1.65 mAh g^{-1} cycle^{-1} at 55 °C.

The in situ XRD patterns collected during the second charge/discharge cycle for the $Li_{1.06}Mn_2O_{3.94}Cl_{0.06}$ cathode are shown in Fig. 6. All the diffraction peaks shift gradually to larger angles as the cells were charged to higher voltages. Reverse shifting is manifested for the cells discharged and quasi-equilibrated at various voltages. From the fully charged state to 4.200 V, the spinel host accomdates Li$^+$ ions as a single-phase of λ-MnO$_2$. Two-phase coexistence is observed in the samples quasi-equilibrated at 4.150 V for discharging and 4.175 V for charging processes. Then a continuous solid solution is observed at voltages lower than 4.125 V. The results are
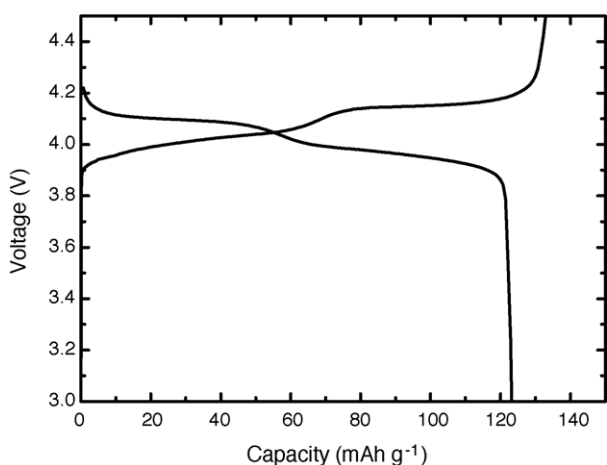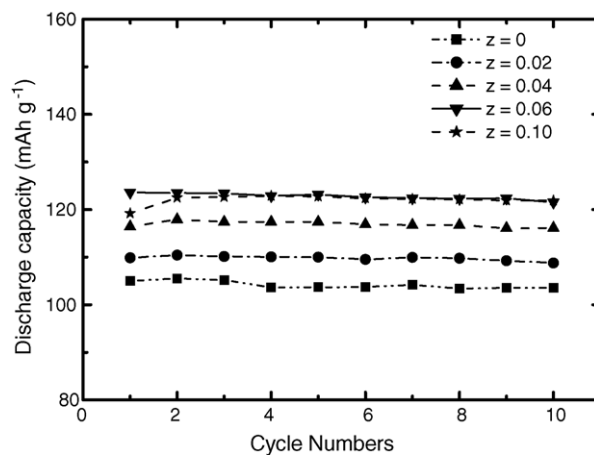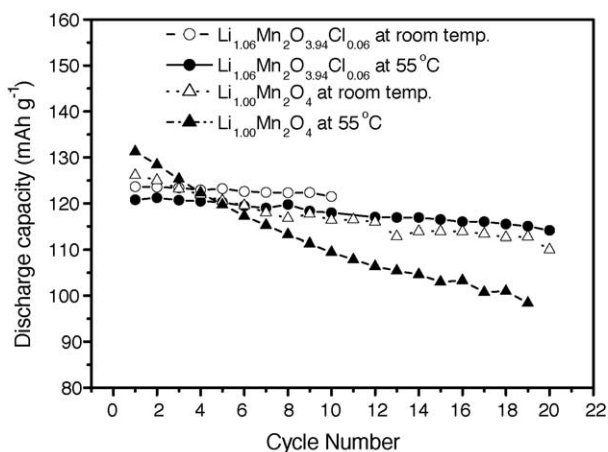

Fig. 3. The initial charge/discharge curves of the $Li_{1.06}Mn_2O_{3.94}Cl_{0.06}$ cathode performed with constant current of 0.1 mA (about C/3).

Fig. 5. Variations of discharge capacity with cycle number for cells with $LiMn_2O_4$ or $Li_{1.06}Mn_2O_{3.94}Cl_{0.06}$ cathode in 1 M LiPF$_6$ in EC:DEC (1:1 V) electrolyte at 55 °C.
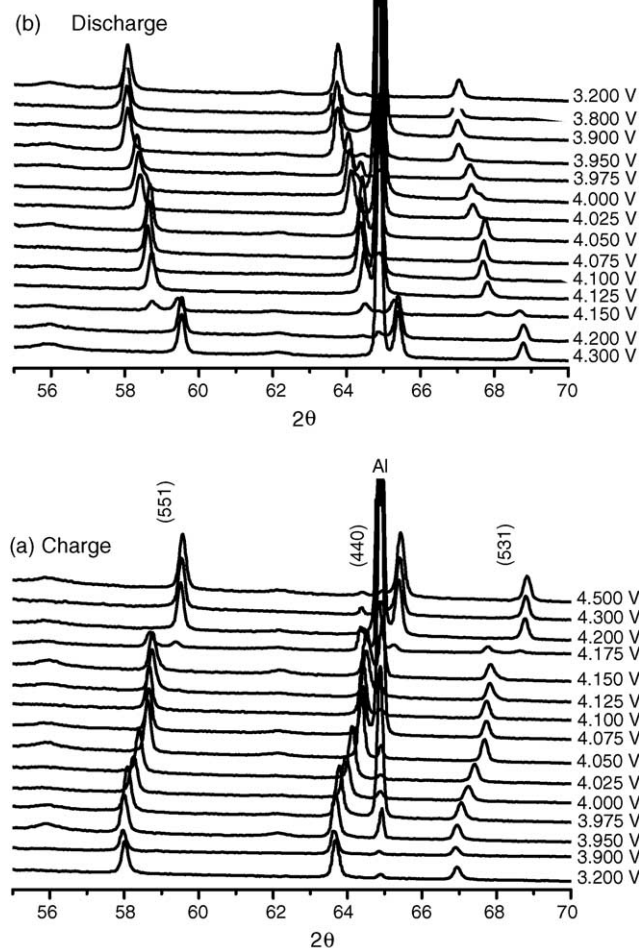
Fig. 6. In situ XRD patterns of the $Li_{1.06}Mn_2O_{3.94}Cl_{0.06}$ cathode quasi-equilibrated at various voltages during the second charge/discharge cycle.

Fig. 7. Variation of cubic lattice parameter of $Li_{1.06}Mn_2O_{3.94}Cl_{0.06}$ cathode with voltage at which in situ cell was quasi-equilibrated during the second cycle.

similar to those performed with in situ XRD by cells cycled at a slow rate for spinel $LiMn_2O_4$ and $LiMn_2O_{4-y}F_y$ reported previously [22,23]. Two-phase region was only found in the lithium concentration, x, range of 0.15–0.35 for $Li_xMn_2O_4$ and 0.25–0.5 for $Li_xMn_2O_{3.74}F_{0.26}$. However, it is different from the results of ex situ or in situ XRD studies for $LiMn_2O_4$ spinel that two distinct phase transitions occur in the vicinity of 4.0 and 4.1 V for cell continuously charged or discharged with fast rate [11,24,25]. The existence of the diffraction peaks of two phases at 4.0 V region may be contributed by different lithium concentrations occur on the surface and at the core of cathode powders as the cells were cycled with high rates. It had also been found by Berg et al. that a single-phase composition around 4.1 V by in situ neutron diffraction with cell close to equilibrium condition at various potentials by raising potential in steps of 0.05 V [26,27]. They might miss the coexistence of two phases by large potential step since the voltage range for the two-phase coexistence is so narrow. The variation in the lattice parameter with voltage at which cells quasi-equilibrated is plotted in Fig. 7. Highly reversible
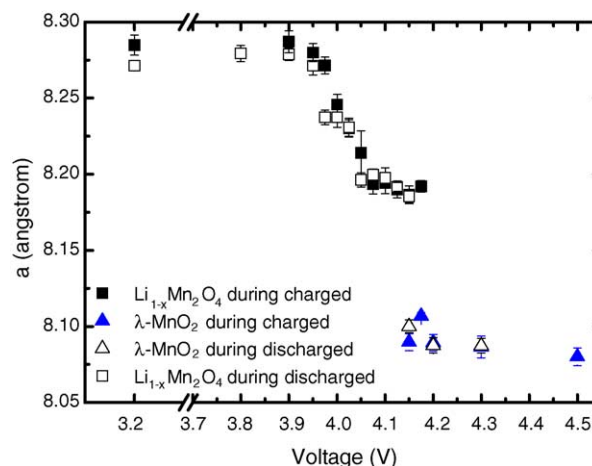
structure during charge–discharge is observed. That may induce the cathode material exhibit excellent cycleability at ambient and high temperatures, though large lattice parameter difference, $\Delta a = 0.08$ Å, between two cubic phases in the two-phase region is determined.

4. Conclusions

Partially chlorine substituted spinel $Li_{1.06}Mn_2O_{4-z}Cl_z$, $0 \le z \le 0.10$, were prepared successfully with citrate gel method. Among the prepared samples, spinel oxychloride with composition of $Li_{1.06}Mn_2O_{3.94}Cl_{0.06}$ shows initial specific discharge capacity of 123 mAh g^{-1} which is higher than that of others. The sample does not only exhibit excellent cycleability at ambient temperature but also show improved cycling performance at 55 °C. It may be caused by the structure of the sample manifest high reversibility during charge–discharge.

Acknowledgements

References

[1] M.M. Thackeray, P.J. Johnson, L.A. de Piccioto, P.G. Bruce, J.B. Goodenough, Mater. Res. Bull. 19 (1984) 179.
[2] J.M. Tarascon, D. Guyomard, J. Electrochem. Soc. 138 (1991) 2864.
[3] T. Ohzuku, A. Ueda, M. Nagayama, J. Electrochem. Soc. 140 (1993) 1862.
[4] Y. Xia, M. Yoshio, J. Power Sources 66 (1997) 129.
[5] Y. Xia, Y. Zhou, M. Yoshio, J. Electrochem. Soc. 144 (1997) 2593.
[6] D.H. Jang, Y.J. Shin, S.M. Oh, J. Electrochem. Soc. 143 (1996) 2204.

[7] A. Du Pasquier, A. Blyr, P. Courjal, D. Larcher, G. Amatucci, B. Gérand, J.-M. Tarascon, J. Electrochem. Soc. 146 (1999) 428.

[8] R. Premanand, A. Durairajan, B. Haran, R. White, B. Popov, J. Electrochem. Soc. 149 (2002) A54.

[9] J.M. Tarascon, E. Wang, F.K. Shokoohi, W.R. McKinnon, S. Colson, J. Electrochem. Soc. 138 (1991) 2859.

[10] R.J. Gummow, A. de Kock, M.M. Thackeray, Solid State Ionics 69 (1994) 59.

[11] Y. Xia, M. Yoshio, J. Electrochem. Soc. 143 (1996) 825.

[12] A.D. Robertson, S.H. Lu, W.F. Averill, W.F. Howard Jr., J. Electrochem. Soc. 144 (1997) 3500.

[13] Y. Xia, Y. Hideshima, N. Kumada, M. Nagano, M. Yoshio, J. Power Sources 24 (1998) 24.

[14] J.H. Lee, J.K. Hong, D.H. Jang, Y.-K. Sun, S.M. Oh, J. Power Sources 89 (2000) 7.

[15] G.G. Amatucci, N. Pereira, T. Zheng, J.-M. Tarascon, J. Electrochem. Soc. 148 (2001) A171.

[16] G.G. Amatucci, N. Pereira, T. Zheng, I. Plitz, J.M. Tarascon, J. Power Sources 81/82 (1999) 39.

[17] Y.-K. Sun, Y.-S. Jeon, J. Mater. Chem. 9 (1999) 3147.

[18] Y.-K. Sun, Electrochem. Commun. 2 (2000) 6.

[19] Y.-K. Sun, Y.-S. Jeon, H.J. Lee, Electrochem. Solid State Lett. 3 (2000) 7.

[20] Y.-K. Sun, Y.-S. Lee, M. Yoshio, Mater. Lett. 56 (2002) 418.

[21] S.-H. Kang, J.B. Goodenough, J. Electrochem. Soc. 147 (2000) 3621.

[22] W. Liu, K. Kowal, G.C. Farrington, J. Electrochem. Soc. 145 (1998) 459.

[23] M.R. Palacín, F. Le Cras, L. Seguin, M. Anne, Y. Chabre, J.M. Tarascon, G. Amatucci, G. Vaughan, P. Strobel, J. Solid State Chem. 144 (1999) 361.

[24] Y.J. Lee, F. Wang, S. Mukerjee, J. McBreen, C.P. Grey, J. Electrochem. Soc. 147 (2000) 803.

[25] E. Levi, M.D. Levi, G. Salitra, D. Aurbach, R. Oesten, U. Heider, L. Heider, Solid State Ionics 126 (1999) 109.

[26] H. Berg, J.O. Thomas, Solid State Ionics 126 (1999) 227.

[27] H. Berg, H. Rundlöv, J.O. Thomas, Solid State Ionics 144 (2001) 65.